Optical and Quantum Electronics (2019) 51:398
https://doi.org/10.1007/s11082-019-2119-y

# Self-focusing of cosh-Gaussian laser beam and its effect on the excitation of ion-acoustic wave and stimulated Brillouin backscattering in collisionless plasma

**Gunjan Purohit**[1] · **Bineet Gaur**[1]

Received: 2 June 2019 / Accepted: 15 November 2019 / Published online: 20 November 2019


**Abstract**

An analytical and numerical study has been carried out for self-focusing of an intense cosh-Gaussian laser beam in collisionless plasma and its impact on the excitation of ion-acoustic wave and stimulated Brillouin backscattering process. The analytical model has been developed under Wentzel–Kramers–Brillouin and paraxial ray approximations. The nonlinearities of ponderomotive force on electron and the relativistic oscillation of the electron mass have been used in this study. The nonlinear differential equations have been set up for the beam width parameters of the main beam, ion-acoustic wave, backscattered wave and back reflectivity of stimulated Brillouin scattering (SBS). These equations have been solved numerically for different values of decentred parameter ($b$), relative plasma density ($\omega_{p0}/\omega_0$) and incident laser intensity ($a$). The results have been compared with only relativistic nonlinearity and Gaussian profile of laser beam. The focusing of laser beam, ion-acoustic wave and scattered wave are found to be strong under relativistic-ponderomotive regime compared to only relativistic regime. Further, it is observed that focusing/intensity of main laser beam, ion acoustic wave and SBS back reflectivity increases with increasing the values of $b$ and $\omega_{p0}/\omega_0$. Itis also found that back reflectivity of SBS process gets suppressed with the increase in the value of $a$. This study may be useful in laser induced fusion scheme where back scattering of SBS plays very important role.

**Keywords** Self-focusing · Relativistic-ponderomotive nonlinearity · Collisionless plasma · Cosh-Gaussian laser beam · Ion-acoustic wave · Stimulated Brillouin scattering

## 1 Introduction

Stimulated Brillouin scattering (SBS) of laser radiation in plasmas is a parametric process which describes the decay of the incident high-power laser radiation into the scattered electromagnetic wave and low frequency ion-acoustic wave (Kruer 1988). The incident laser flux becomes depleting and redirecting in this process. It is one of the most important

✉ Gunjan Purohit
gunjan75@gmail.com

[1] Laser Plasma Computational Laboratory, Department of Physics, DAV (PG) College, Dehradun, Uttarakhand 248001, India

parametric instability in laser plasma interaction, which plays an important role in inertial confinement fusion (ICF) scheme (Labaune et al. 1997; Neumayer et al. 2008). This instability may grow in the entire subcritical density region of the plasma resulting in a large amount of backscattered laser radiation. SBS reduce the laser plasma coupling efficiency and modify uniformity of energy deposition. Further, the uniformity of energy deposition inside the plasma is also affected by self-focusing/filamentation of laser beam (Kaw et al. 1973; Wei et al. 2004; Varaki and Jafari 2017; Gupta and Singh 2017; Thakur and Kant 2019). Self-focusing and stimulated Brillouin scattering of laser beam become greatly affected the laser plasma coupling. Therefore, the suppression of filamentation and stimulated Brillouin scattering of an intense laser beam in plasma are two important issues for the success of ICF scheme.

Stimulated Brillouin scattering of an intense self-focused/filamented laser beam in plasma has been studied to a great extent in the past (Aleksandrov et al. 1985; Rozmus et al. 1987; Mahmoud et al. 1999; Giulietti et al. 1999; Sharma et al. 2009; Gao et al. 2010; Niknam et al. 2013; Singh and Walia 2013; Masson-Laborde et al. 2014; Purohit and Rawat 2015). These investigations suggest that SBS is a harmful process that limits the pulse energy of high-power laser sources. The back reflectivity of SBS depend strongly on the intensity of the incident laser beam, plasma density and electron temperature (where $T_i \ll T_e$). The backscattering of SBS process becomes affected by self-focused pump laser beam and ion-acoustic wave. It has been found that when pump laser beam propagating into the plasma, beam loses coherence due to self-focusing (Myatt et al. 2001; Fuchs et al. 2001). The SBS instability becomes affected by this incoherence. It has been reported that the filamentation of laser beam may strongly influence the temporal evolution of SBS, the amount and direction of the scattered light (Amin et al. 1993; Eliseev et al. 1995). Giulietti et al. (1999) have performed an experimental study of stimulated Brillouin backscattering from the interaction of a laser pulse with a long-scale-length, expanding plasma in a regime favourable to strong self-focusing/filamentation. Their results show a strong effect of dynamical self-focusing on back SBS. Baldis et al. (1993) have presented an experimental and theoretical study of SBS in laser produced plasma using a picosecond laser pulse. An experimental study of the dependence of the SBS reflectivity on the focusing aperture and the incident laser intensity has been carried out by Baton et al. (1998). They found that the saturation level of SBS reflectivities was of the order of 10%. Labaune et al. (1991) have measured the reflectivity of SBS from an underdense homogeneous plasma irradiated by a picosecond laser pulse. In Mounaix et al. (2000) have studied analytically the effect of laser beam smoothing on stimulated Brillouin backscattering in the limit of the independent hot spot model and found that the temporal beam smoothing can reduce the back reflectivity of SBS significantly. In the work of Huller et al. (2008), numerical simulation of SBS have been investigated for an intense mono-speckle laser beams in expanding plasmas. They found very good agreement between the theoretical numerical modelling and the experimental results, particularly for the SBS activity in the plasma and the backscatter level. Niknam et al. (2013) have investigated the effects of relativistic mass and ponderomotive nonlinearities on self-focusing and stimulated Brillouin back-scattering of a long intense laser pulse in a finite temperature relativistic plasma. Their results show that the growth rate of SBS backscattered wave increases by increasing the values of electron density and temperature. The effect of ponderomotive self -focusing (filamentation) of the laser beam on the localization of ion acoustic wave (IAW) and on SBS process have been studied by Sharma et al. (2009). They showed that back reflectivity of SBS process gets suppressed. Singh and Walia (2013) have investigated the effect of self-focused Gaussian laser on SBS process in collisionless plasma under ponderomotive nonlinearity using moment theory and paraxial-ray approximation. They found that back reflectivity of SBS is less in moment theory approach as compared to paraxial theory approach. Other important studies of SBS process in laser plasma interaction have been found in the literature (Labaune et al. 1985, 1996; Chirokikh et al. 1998; Wang et al. 2009; Yahia et al. 2015; Albright et al. 2016).

Self-focusing and SBS process of an intense laser beam in the plasma depends on the spatial intensity profile of laser beams as well as nonlinearities associated with them. Self-focusing of an intense laser beam in the plasma is an intensity-dependent changes in the plasma index of refraction, which is mainly due to ponderomotive and relativistic nonlinearities. Due to self-focusing of intense laser beam in the plasma, there may be reduction in the plasma density by ponderomotive expulsion of electrons and ions, or a reduction in the plasma frequency due to relativistic mass increase of electrons. Self-focusing/filamentation instability of an intense laser at high plasma densities has been a main motivation for studying the utility of SBS process. In most of earlier work on self-focusing and SBS instability in laser plasma interaction, the effect of ponderomotive and relativistic nonlinearity have been taken separately. An ultra-intense laser pulse may generate different types of nonlinearities at different timescales in the plasma (Borisov et al. 1992; Brandi et al. 1993a, b). When $\tau_{pe} < \tau < \tau_{pi}$ (where $\tau_{is}$ the laser-pulse duration, $\tau_{pi}$ is the ion plasma period, and $\tau_{pe}$ is the electron plasma period), relativistic and ponderomotive nonlinearities are operative. These nonlinearities contribute to focusing on femtosecond time scale. The combined effect of ponderomotive and relativistic nonlinearities on self-focusing and SBS process have been found in few studies (Niknam et al. 2013; Gauniyal et al. 2017). Moreover, different intensity profiles of laser beams such as Gaussian, ring-rippled, super Gaussian, hollow Gaussian, elliptical, cosh-Gaussian etc. behave differently in plasmas. Except of Gaussian profile of laser beams, other profiles have been less used in the study of self-focusing and SBS process. In particular the cosh-Gaussian intensity profile of a laser beam (decentred Gaussian beams) have evinced the great interest due to its unique propagation properties and attractive applications (Lu and Luo 2000; Zhou 2011; Gill et al. 2011; Nanda and Kant 2014; Habibi and Ghamari 2015). The cosh-Gaussian laser beams can be produced by the superposition of two decentered laser beams that are having same spot size and are in phase with each other. In the laboratory, such decentered laser beams can be produced by reflection of Gaussian laser beams from a spherical mirror whose centre is offset from a beam axis (Al-Rashed and Saleh 1995). These beams having higher efficient power in comparison to the Gaussian laser beam (Konar et al. 2007). One of the important characteristics of cosh-Gaussian laser beams is that they may be focused at a desired position by choosing a suitable decentred parameter.

This paper investigates self-focusing of an intense cosh-Gaussian laser beam in collisionless plasma and its effect on the excitation of ion-acoustic wave and stimulated Brillouin back scattering process. This study has been carried out in the presence of relativistic and ponderomotive nonlinearities. Paraxial ray theory (Sodha et al. 1974; Akhmanov et al. 1968) have been used in this study, which is based on the expansion of the eikonal and nonlinear dielectric constant up to square term $r^2$, where $r$ is the distance from the axis of beam. The results have been compared with Gaussian profile of laser beam and only relativistic nonlinearity. Suitable set of laser and plasma parameters have been taken in this study. In Sect. 2, we have derived the equations for the effective dielectric constant of the plasma and the beam width parameter for cosh-Gaussian beam propagating in the plasmas using WKB and paraxial-ray approximations, when relativistic and ponderomotive nonlinearities are operative. Section 3 describes the equations for the excitation of ion-acoustic wave in presence of relativistic-ponderomotive nonlinearity. The equations that govern the dynamics of SBS process and back reflectivity of

SBS have been derived in Sect. 4. The numerical results have been discussed in Sect. 5 and the conclusions of the present work are summarized in Sect. 6.

## 2 Analytical formulation

We consider the propagation of an intense cosh-Gaussian laser beam of frequency $\omega_0$ along the $z$-direction in collisionless plasma. The field distribution of the beam propagating in the plasma along $z$-axis is given by (Casperson et al. 1997; Lu et al. 1999; Nanda and Kant 2014)

$$E(r,z) = \frac{E_0}{2f} \exp\left(\frac{b^2}{4}\right)\left[\exp\left\{-\left(\frac{r}{r_0 f} + \frac{b}{2}\right)^2\right\} + \exp\left\{-\left(\frac{r}{r_0 f} - \frac{b}{2}\right)^2\right\}\right] \tag{1}$$

where $r$ is the radial coordinate of the cylindrical coordinate system, $r_0$ is the initial beam width, $b$ is the decentred parameter of the beam, $f$ is the dimensionless beam width parameter of the laser beam in plasma which is unity at $z=0$, and $E_0$ is the amplitude of cosh-Gaussian laser beam for the central position at $r=z=0$.

### 2.1 Effective dielectric constant of the plasma

The effective dielectric constant of the plasma at frequency $\omega_0$ is given by

$$\varepsilon = \varepsilon_0 + \phi(E \cdot E^*) \tag{2}$$

where $\varepsilon_0$ and $\phi(E{\cdot}E^*)$ represent the linear and nonlinear parts of dielectric constant respectively. The linear part of dielectric constant of the plasma can be expressed as

$$\varepsilon_0 = 1 - \frac{\omega_{p0}^2}{\omega_0^2} \tag{3}$$

where $\omega_{p0}$ and $\omega_0$ are the relativistic electron plasma frequency given by $\omega_{p0} = \frac{4\pi n_0 e^2}{m_0 \gamma_0}$ and the pump wave frequency (with $e$ is the charge of an electron, $m_0$ its rest mass and $n_0$ is the density of plasma electrons in the absence of laser beam) respectively. The relativistic factor $\gamma_0$ can be written as

$$\gamma_0 = (1 + \alpha E \cdot E^*)^{\frac{1}{2}} \tag{4}$$

where $\alpha = \frac{e^2}{c^2 m_0^2 \omega_0^2}$.

The relativistic-ponderomotive force is given by (Borisov et al. 1992; Brandi et al. 1993a, b)

$$F_P = -m_0 c^2 \nabla\left(\gamma_0 - 1\right). \tag{5}$$

The electron density in the plasma can be written as

$$n_e = n_0 + n_2 \tag{6}$$

where $n_2$ is the modified electron density due to the ponderomotive force and is given by (Brandi et al. 1993a, b)

$$n_2 = n_0\left[\frac{c^2}{\omega_{p0}^2}\left(\nabla^2\gamma - \frac{(\nabla\gamma)^2}{\gamma}\right)\right] \tag{7}$$

and

$$\begin{aligned}\frac{n_e}{n_0} =& 1 + \frac{c^2 a}{\omega_{p0}^2 4f^2}\left[\left(1 + \frac{e^2}{c^2 m_0^2\omega_0^2}E\cdot E^*\right)^{-\frac{1}{2}} XY + \left(1 + \frac{e^2}{c^2 m_0^2\omega_0^2}E\cdot E^*\right)^{-\frac{1}{2}} r^2 Y^2\right] \\ &- \frac{2a}{4f^2}\left(1 + \frac{e^2}{c^2 m_0^2\omega_0^2}E\cdot E^*\right)^{-\frac{3}{2}} X^2 r^2 Z^2\end{aligned} \tag{8}$$

where $a = \alpha E_0^2$ is the intensity parameter,

$$X = \exp\left[-\left(\frac{r^2}{r_0^2 f^2} + \frac{br}{r_0 f}\right)\right] + \exp\left[-\left(\frac{r^2}{r_0^2 f^2} - \frac{br}{r_0 f}\right)\right]$$

$$Y = \exp\left[-\left(\frac{r^2}{r_0^2 f^2} + \frac{br}{r_0 f}\right)\right]\left(-\frac{2}{r_0^2 f^2} - \frac{b}{r r_0 f}\right) + \exp\left[-\left(\frac{r^2}{r_0^2 f^2} - \frac{br}{r_0 f}\right)\right]\left(-\frac{2}{r_0^2 f^2} + \frac{b}{r r_0 f}\right)$$

and

$$\begin{aligned}Z =& \exp\left[-\left(\frac{r^2}{r_0^2 f^2} + \frac{br}{r_0 f}\right)\right]\left(-\frac{4}{r_0^2 f^2} - \frac{b}{r r_0 f} + \frac{4r^2}{r_0^4 f^4} + \frac{b^2}{r_0^2 f^2} + \frac{4br}{r_0^3 f^3}\right) \\ &+ \exp\left[-\left(\frac{r^2}{r_0^2 f^2} - \frac{br}{r_0 f}\right)\right]\left(-\frac{4}{r_0^2 f^2} + \frac{b}{r r_0 f} + \frac{4r^2}{r_0^4 f^4} + \frac{b^2}{r_0^2 f^2} - \frac{4br}{r_0^3 f^3}\right).\end{aligned}$$

The nonlinear part of dielectric constant is given by

$$\phi(E\cdot E^*) = \frac{\omega_{p0}^2}{\omega_0^2}\left(1 - \frac{n_e}{n_0\gamma}\right). \tag{9}$$

Expanding the dielectric constant around $r = 0$ in Eq. (3) by Taylor expansion, one can write

$$\varepsilon = \varepsilon_f + \gamma_1 r^2 \tag{10}$$

where

$$\varepsilon_f = \varepsilon_0 + \frac{\omega_{p0}^2}{\omega_0^2}\left[1 - \frac{1}{\gamma_0} - \frac{c^2 a}{\omega_0^2 f^4 r_0^2}\left(b^2 - 4\right)\right]$$

and

$$\gamma_1 = -\frac{\omega_{p0}^2}{\omega_0^2}\left[\frac{a}{\gamma_0^3 f^4 r_0^2} + \frac{c^2 a}{\omega_{p0}^2 f^2}\left(\frac{\left(16-4b^2\right)}{\gamma_0^2 f^4 r_0^4} + \frac{a\left(2b^2-16\right)}{\gamma_0^4 r_0^4 f^6}\right)\right].$$

### 2.2 Propagation of cosh-Gaussian laser beam in plasma

The propagation of the laser beam in a collisionless plasma is governed by the wave equation

$$\nabla^2 E - \nabla(\nabla \cdot E) + \frac{\omega_0^2}{c^2}\varepsilon E = 0 \tag{11}$$

where $\varepsilon$ is the effective dielectric function of the plasma and $c$ is the velocity of light.

The second term on left hand side of Eq. (11) can be neglected under WKB approximation (Sodha et al. 1974). The solution of Eq. (11) can be written as

$$E = A(r,z)\exp(-ik_0 z) \tag{12}$$

where $A(r, z)$ is the slowly varying complex amplitude of the electric field. The complex amplitude $(r, z)$ may be expressed as

$$A(r,z) = A_0(r,z)\exp(-ik_0 S_0) \tag{13}$$

where $A_0$ and $S_0$ are the real function of $r$ and $z$. Substituting Eqs. (12) and (13) into Eq. (11) and separating the real and imaginary parts, we get

$$2\frac{\partial S_0}{\partial z} + \left(\frac{\partial S_0}{\partial z}\right)^2 = \frac{1}{k_0^2 A_0}\left(\frac{\partial^2}{\partial r^2} + \frac{\partial^2}{\partial z^2} + \frac{1}{r}\frac{\partial}{\partial r}\right)A_0 + \frac{\omega_0^2}{k_0^2 c^2}\varepsilon \tag{14}$$

and

$$\frac{\partial A_0^2}{\partial z} + \frac{\partial A_0^2}{\partial r}\frac{\partial S_0}{\partial r} + A_0^2\left(\frac{1}{r}\frac{\partial}{\partial r} + \frac{\partial^2 S_0}{\partial r^2}\right) = 0. \tag{15}$$

The solution of the above coupled equations can be written as (Sodha et al. 1974; Akhmanov et al. 1968)

$$S_0 = \phi_0(z) + \frac{r^2}{2}\beta_0(z)$$

$$\beta_0(z) = \frac{1}{f(z)}\frac{df(z)}{dz}$$

and the laser beam intensity is given by

$$A_0^2 = \frac{E_0^2}{4f^2}\exp\left(\frac{b^2}{2}\right)\left[\exp\left\{-\left(\frac{r}{r_0 f} + \frac{b}{2}\right)^2\right\} + \exp\left\{-\left(\frac{r}{r_0 f} - \frac{b}{2}\right)^2\right\}\right]^2. \tag{16}$$

Substituting Eq. (16) in Eq. (14) and equating the coefficients of $r^2$ on both sides, the laser beam width parameter $f$ is given by

$$\frac{d^2f}{d\xi^2} = \left(\frac{12-12b^2-b^4}{3f^3}\right) - \left[\left(\frac{\omega_{p0}^2 r_0^2}{c^2}\right)\frac{a}{\gamma_0^3 f^3} + \frac{a}{f}\left(\frac{\left(16-4b^2\right)}{\gamma_0^2 f^4} + \frac{a\left(2b^2-16\right)}{\gamma_0^4 f^6}\right)\right] \tag{17}$$

where $\xi(=z/k_0r^2)$ is the dimensionless distance of propagation. Equation (16) shows the variation of beam width in plasma, when both relativistic and ponderomotive nonlinearities are operative. The first term on right hand side is responsible for diffractional divergence of the laser beam, and the second term is the nonlinear term which arises due to relativistic-ponderomotive force and is responsible for focusing/defocusing of laser beam in plasma.

## 3 Generation of ion-acoustic wave

The background density of the plasma gets modified due to ponderomotive force and relativistic effect and the laser beam becomes self-focused/filamented. The laser beam exhibits a steep intensity gradient in the transverse direction, which generate an ion-acoustic wave at pump frequency. The ion-acoustic wave is excited due to nonlinear coupling of intense cosh-Gaussian laser beam with modified density of plasma. The magnitude of this ion-acoustic wave can be obtained by using the equation of continuity, equation of motion and Poisson's equation. Using these equations, one obtains the following equation for the ion density variation (Gauniyal et al. 2017)

$$\frac{\partial^2 n_{i0}}{\partial t^2} + 2\Gamma_i\frac{\partial n_{i0}}{\partial t} - \gamma_i v_{th}^2\nabla^2 n_{i0} + \frac{\omega_{p0}^2}{\gamma}\frac{n_e}{n_0}\frac{k_i^2\lambda_d^2}{1+k_i^2\lambda_d^2}n_{i0} = 0 \tag{18}$$

where $v_{th} = \frac{k_BT_i}{m_i}$ is the thermal velocity of ions, $\gamma_i$ is the ratio of specific heat of ion-gas, and $\lambda_d = \left(\frac{k_BT_0}{4\pi n_0e^2}\right)^{1/2}$ is the Debye length. The Landau damping coefficient ($2\Gamma_i$) for ion acoustic wave is given by (Krall and Trivelpicec 1973)

$$2\Gamma_i = \frac{k_i}{(1+k_i^2\lambda_d^2)}\left(\frac{\pi k_BT_e}{8m_i}\right)^{1/2} \times \left[\left(\frac{m}{m_i}\right)^{1/2} + \left(\frac{T_e}{T_i}\right)^{3/2}\exp\left\{-\frac{T_e}{T_i(1+k_i^2\lambda_d^2)}\right\}\right] \tag{19}$$

where $k_i$ is the wave vector of the ion-acoustic wave, $T_e$ and $T_i$ are the electron and ion temperatures ($T_e \gg T_i$), $m_i$ is the ionic mass and other symbols have their usual meaning. The relation between perturbation in the electron and ion densities is given by

$$n_{e0} = n_{i0}\left[1 + \frac{k_i^2\lambda_d^2}{(n_e/n_0\gamma)}\right]^{-1} \tag{20}$$

where $n_{i0}$ and $n_{e0}$ are the perturbation in the ion and electron density.

The solution of Eq. (18) can be written as

$$n_{i0} = n_i(r,z)\exp\{i[\omega_i t - k_i(z + S_i(r,z))]\} \tag{21}$$

where $n_i$ is the slowly varying real function for $r$ and $z$ and $S_i$ is the eikonal for the ion-acoustic wave. The frequency ($\omega_i$) and wave number ($k_i$) of the ion-acoustic wave satisfy the Bohm-Gross dispersion relation

$$\omega_i^2 = \frac{k_i^2 c_s^2}{1 + k_i^2 \lambda_d^2 (n_e/n_0\gamma)^{-1}} \tag{22}$$

where $c_s = \frac{k_B T_e}{m_i}$ is the speed of ion-acoustic wave.

Substituting Eq. (21) into (18) and separating the real and imaginary parts, one obtains

$$2\frac{\partial S_i}{\partial z} + \left(\frac{\partial S_i}{\partial r}\right)^2 = \frac{1}{k_i^2 n_i}\left(\frac{\partial^2 n_i}{\partial r^2} + \frac{1}{r}\frac{\partial n_i}{\partial r}\right) + \frac{\omega_i^2}{k_i^2 c_s^2}\left(1 - \frac{1}{1 + k_i^2\lambda_d^2\left(\frac{n_e}{n_0\gamma}\right)^{-1}}\right) \tag{23}$$

and

$$\frac{\partial n_i^2}{\partial z} + \left(\frac{1}{r}\frac{\partial S_i}{\partial r} + \frac{\partial^2 S_i}{\partial r^2}\right)n_i^2 + \frac{\partial n_i^2}{\partial r}\frac{\partial S_i}{\partial r} + \frac{2\Gamma_i\omega_i}{k_i c_s^2}n_i^2 = 0. \tag{24}$$

The solution of Eqs. (23) and (24) can be written as (Sodha et al. 1974; Akhmanov et al. 1968)

$$n_i^2 = \frac{n_{00}^2}{4f_i^2}\exp\left(\frac{b^2}{2}\right)\left[\exp\left\{-\left(\frac{r}{a_i f_i} + \frac{b}{2}\right)^2\right\} + \exp\left\{-\left(\frac{r}{a_i f_i} - \frac{b}{2}\right)^2\right\}\right]^2 \exp(-2k_{i0}z) \tag{25}$$

and

$$S = \frac{r^2}{2f}\frac{df_i}{dz} + \phi_i(z) \tag{26}$$

where $k_{i0}(= \Gamma_i\omega/k_i c_s^2)$ is the damping factor, $n_{00}$ and $a_i$ are the axial amplitude of density perturbation and the initial beam width of ion-acoustic wave, and $f_i$ is a dimensionless beam width parameter of ion-acoustic wave. Substituting Eqs. (25) and (26) in Eq. (23) and equating the coefficients of $r^2$ on both sides, we obtain the following equation for $f_i$:

$$\begin{aligned}\frac{d^2 f_i}{d\xi^2} = &\left(\frac{12 - 12b^2 - b^4}{3f_i^3}\right)\frac{r_o^4}{a_i^4} - \frac{f_i}{\gamma_i}\left(\frac{c^2}{v_{th}^2}\right)\\ &\left[\left(\frac{\omega_{p0}^2 r_0^2}{c^2}\right)\frac{a}{\gamma_0^3 f^4} + \frac{a}{f}\left(\frac{(16 - 4b^2)}{\gamma_0^2 f^6} + \frac{a(2b^2 - 16)}{\gamma_0^4 f^8}\right)\right]\frac{k_i^2\lambda_d^2}{(1 + k_i^2\lambda_d^2)^2}\end{aligned} \tag{27}$$

Equation (27) describes the beam width parameter ($f_i$) of the ion acoustic wave in collision less plasma. The initial conditions for $f_i$ are $df_i/dz = 0$, and $f_i = 1$ at $z = 0$.

## 4 Stimulated Brillouin scattering

The nonlinear coupling between high power laser beam with the low frequency mode of the plasma i.e. ion-acoustic wave having frequency $\omega_i$ and wave number $k_i$ results in stimulated Brillouin scattering of frequency $\omega_s$ and wave number $k_s$. The total electric field $E_H$ i.e. sum of the electric field $E_0$ of the pump laser beam and of the electric field $E_S$ of the scattered wave in the plasma may be expressed as

$$E_H = E_0 \exp(i\omega_0 t) + E_S \exp(i\omega_S t). \tag{28}$$

The high frequency electric field $E_H$ satisfy the following wave equation

$$\nabla^2 E_H - \nabla(\nabla \cdot E_H) = \frac{1}{c^2}\frac{\partial^2 E_H}{\partial t^2} + \frac{4\pi}{c^2}\frac{\partial J_T}{\partial t} \tag{29}$$

where $J_T$ is the current density vector. Substituting Eq. (28) into Eq. (29), and separating the equation for pump and scattered field

$$\nabla^2 E_0 + \frac{\omega_0^2}{c^2}\left[1 - \left(\frac{n_e}{n_0}\right)\frac{\omega_{p0}^2}{\gamma\omega_S^2}\right]E_0 = -\frac{2\pi e i\omega_0}{c^2}(n_{e0}v_0) \tag{30}$$

and

$$\nabla^2 E_S + \frac{\omega_s^2}{c^2}\left[1 - \left(\frac{n_e}{n_0}\right)\frac{\omega_{p0}^2}{\gamma\omega_S^2}\right]E_S = -\frac{2\pi e i\omega_s}{c^2}(n_{e0}^* v_s). \tag{31}$$

In order to solve Eq. (31), the term $\nabla(\nabla \times E_T)$ may be neglected in the comparison to the $\nabla^2 E_S$. Substituting $v_s = ieE_0/m\omega_0$ into Eq. (31), one obtains the wave equation for the scattered field

$$\nabla^2 E_S + \frac{\omega_s^2}{c^2}\left[1 - \left(\frac{n_e}{n_0}\right)\frac{\omega_{p0}^2}{\gamma\omega_S^2}\right]E_S = \frac{1}{2}\frac{\omega_{p0}^2}{c^2}\frac{\omega_s}{\omega_0}\frac{n_{e0}^*}{n_0}E_0. \tag{32}$$

The solution of Eq. (32) can be written as

$$E_S = E_{S0}(r,z)\exp(ik_{S0}z) + E_{S1}(r,z)\exp(-ik_{S1}z) \tag{33}$$

where $E_{S0}$ and $E_{S1}$ are the slowly varying real functions of $r$ and $z$ and $k_{S0}$ and $k_{S1}$ are the propagation constants of scattered wave. $k_{S1}$ and $\omega_s$ satisfy the phase matching conditions i.e. $\omega_s = \omega_0 - \omega_i$ and $k_{S1} = k_0 - k_i$ and

$$k_{S0}^2 = \frac{\omega_s^2}{c^2}\left(1 - \frac{\omega_{p0}^2}{\omega_s^2}\right) = \frac{\omega_s^2}{c^2}\varepsilon_{S0}.$$

Using Eq. (33) in (32) and separating terms with different phases, one gets

$$-k_{S0}^2 E_{S0} + 2ik_{S0}\frac{\partial E_{S0}}{\partial z} + \left(\frac{\partial^2}{\partial r^2} + \frac{1}{r}\frac{\partial}{\partial r}\right)E_{S0} + \frac{\omega_s^2}{c^2}\varepsilon_S(r,z)E_{S0} = 0 \tag{34}$$

$$-k_{S1}^2 E_{S1} - 2ik_{S1}\frac{\partial E_{S1}}{\partial z} + \left(\frac{\partial^2}{\partial r^2} + \frac{1}{r}\frac{\partial}{\partial r}\right)E_{S1} + \frac{\omega_s^2}{c^2}\varepsilon_S(r,z)E_{S1} = \frac{1}{2}\frac{\omega_{p0}^2}{c^2}\frac{\omega_s}{\omega_0}\frac{n_{e0}^*}{n_0}E_0 e^{-ik_0 S_0} \tag{35}$$

where $\varepsilon_S(r,z) = \varepsilon_{S0} + \frac{\omega_{p0}^2}{\omega_s^2}\left(1 - \frac{n_e}{n_0\gamma}\right)$.

The solution for Eq. (35) may be written as

$$E_{S1} = E_{S1}^{'}(r,z)\exp(-ik_0 S_0). \tag{36}$$

Substituting Eq. (36) into (35) and neglecting terms containing space derivatives, we obtain

$$E_{S1}^{\prime} \cong -\frac{1}{2}\frac{\omega_{p0}^2}{c^2}\frac{n_{e0}^*}{n_0}\frac{\omega_s}{\omega_0}\frac{\hat{E}E_0}{\left[k_{S1}^2 - k_{S0}^2 - \frac{\omega_{p0}^2}{c^2}\left(1 - \frac{n_e}{n_0\gamma}\right)\right]} \tag{37}$$

where $\hat{E}$ is a unit vector along $E$.

Substituting $E_{S0} = E_{S00}(r,z)\exp(ik_{S0}S_c)$ in Eq. (34) and separating the real and imaginary parts, one can obtain

$$2\left(\frac{\partial S_c}{\partial z}\right) + \left(\frac{\partial S_c}{\partial r}\right)^2 = \frac{1}{k_{S0}^2 E_{S00}}\left(\frac{\partial^2 E_{S00}}{\partial r^2} + \frac{1}{r}\frac{\partial E_{S00}}{\partial r}\right) + \frac{\omega_{p0}^2}{k_{s0}^2 c^2}\left(1 - \frac{n_e}{n_0\gamma}\right) \tag{38}$$

and

$$\frac{\partial E_{S00}^2}{\partial z} + \frac{\partial E_{S00}^2}{\partial r^2}\frac{\partial S_c}{\partial r} + \left(\frac{\partial^2 S_c}{\partial r^2} + \frac{1}{r}\frac{\partial S_c}{\partial r}\right)E_{S00}^2 = 0 \tag{39}$$

where $E_{S00}$ is the real function of $r$ and $z$ and $S_c$ is the eikonal for the scattered wave. The solution of these equations can be written as

$$E_{s00}^2 = \frac{B_1^2}{4f_S^2}\exp\left(\frac{b^2}{2}\right)\left[\exp\left\{-\left(\frac{r}{a_s f_S} + \frac{b}{2}\right)^2\right\} + \exp\left\{-\left(\frac{r}{a_s f_S} - \frac{b}{2}\right)^2\right\}\right] \tag{40}$$

and

$$S_c = \frac{r^2}{2f_S}\frac{df_S}{dz} + \Phi_C(z) \tag{41}$$

where $a_s$ is the initial beam width of the scattered wave, $f_S$ is the dimensionless beam width parameters of the scattered beam and $B_1$ is the amplitude of the scattered beam. Substituting Eqs. (40) and (41) into Eq. (38) and equating the coefficients of $r^2$ on both sides, we get the equation of the spot size of scattered wave as

$$\frac{d^2 f_S}{d\xi^2} = \left(\frac{12 - 12b^2 - b^4}{3f_i^3}\right)\frac{k_0^2 r_o^4}{k_{s0}^2 a_s^4} - f_s\left(\frac{k_0^2}{k_{s0}^2}\right)\left[\left(\frac{\omega_{p0}^2 r_0^2}{c^2}\right)\frac{a}{\gamma_0^3 f^4} + \frac{a}{f}\left(\frac{(16 - 4b^2)}{\gamma_0^2 f^5} + \frac{a(2b^2 - 16)}{\gamma_0^4 f^7}\right)\right]. \tag{42}$$

## 4.1 Expression of back reflectivity

The expressions for $B_1$ and $a_s$ may be obtained by applying suitable boundary conditions. The appropriate boundary condition would be

$$E_S = E_{S0}(r,z)e^{\mathrm{i}k_{S0}z} + E_{S1}(r,z)e^{-ik_{S1}z} = 0 \quad \text{at } z = z_c \tag{43}$$

where $z_c(= L - z)$ is the distance at which amplitude of the scattered wave is zero and $L$ is the interaction length.

Therefore, at $z = z_c$, one obtains

$$B_1 = \frac{1}{2}\left(\frac{\omega_{p0}^2}{c^2}\right)\left(\frac{n_{00}}{n_0}\right)\left(\frac{\omega_s}{\omega_0}\right)\frac{f_S(z_c)}{f_0(z_c)f_i(z_c)}\frac{E_{00}\exp(-k_i z_c)}{\left[k_{S1}^2 - k_{S0}^2 - \frac{\omega_{p0}^2}{c^2}\left(1 - \frac{n_e}{n_0\gamma}\right)\right]}\frac{\exp[-i(k_{S1}z_c + k_0 S_0)]}{\exp[i(k_{S0}S_c + k_{S0}z_c)]} \tag{44}$$

with condition,

$$\frac{1}{a_s^2 f_S^2} = \frac{1}{r_0^2 f_0^2} + \frac{1}{a_i^2 f_i^2}$$

where $f_S(z_c)$, $f_i(z_c)$ and $f(z_c)$ are the values of dimensionless beam width parameter of scattered wave, ion-acoustic wave and incident (pump) wave at $z = z_c$.

Back reflectivity of stimulated Brillouin scattering is defined as the ratio of scattered flux to the incident flux i.e. $R = \left(\frac{|E_S|^2}{|E_0|^2}\right)$ and is given by

$$R = \frac{1}{16}\left(\frac{\omega_{p0}^2}{c^2}\right)^2\left(\frac{n_{00}}{n_0}\right)^2\left(\frac{\omega_s}{\omega_0}\right)^2\exp\left(\frac{b^2}{2}\right)\frac{1}{\left[k_{S1}^2 - k_{S0}^2 - \frac{\omega_{p0}^2}{c^2}\left(1 - \frac{n_e}{n_0\gamma}\right)\right]^2} \times \left(I_1 + I_2 - I_3\right) \tag{45}$$

where

$$I_1 = \frac{f_s^2(z_c)}{f_s^2 f_i^2(z_c) f^2(z_c)}\left[\exp\left\{-\left(\frac{r}{a_1 f_s} + \frac{b}{2}\right)^2\right\} + \exp\left\{-\left(\frac{r}{a_1 f_s} - \frac{b}{2}\right)^2\right\}\right]\exp(-2k_i z_c)$$

$$I_2 = \frac{1}{f^2 f_i^2}\left[\exp\left\{-\left(\frac{r}{a_0 f_i} + \frac{r}{r_0 f} + \frac{b}{2}\right)^2\right\} + \exp\left\{-\left(\frac{r}{a_0 f_i} + \frac{r}{r_0 f} - \frac{b}{2}\right)^2\right\}\right]\exp(-2k_i z_c)$$

and

$$\begin{aligned} I_3 = {} & 2\frac{f_s(z_c)}{f_i(z_c) f(z_c) f_s f_i f}\left[\exp\left\{-\left(\frac{r}{a_1 f_s} + \frac{b}{2}\right)^2\right\} + \exp\left\{-\left(\frac{r}{a_1 f_s} - \frac{b}{2}\right)^2\right\}\right] \\ & \times \left[\exp\left\{-\left(\frac{r}{a_0 f_i} + \frac{r}{r_0 f} + \frac{b}{2}\right)^2\right\} + \exp\left\{-\left(\frac{r}{a_0 f_i} + \frac{r}{r_0 f} - \frac{b}{2}\right)^2\right\}\right] \\ & \times \exp\left[-k_i\left(z + z_c\right)\right] \times \cos\left[\left(k_{s0} + k_{s1}\right)\left(z - z_c\right)\right] \end{aligned}$$

Equation (45) gives an expression for the back reflectivity of stimulated Brillouin scattering process.

## 5 Numerical results and discussion

In this section, an extensive numerical investigation has been performed of the dynamics of stimulated Brillouin scattering by self-focused cosh-Gaussian laser beam in collisionless plasma for the following laser plasma parameters:

$\omega_0 = 1.778 \times 10^{14}$ rad/s, $r_0 = 20$ μm, $\omega_{p0} = 0.3\ \omega_0$, $a_0 =$ μm, $\upsilon_{th} = 0.1c$, $b = 0$, 0.5 and 1, $a = 1$, 1.4 and 1.8. The initial boundary conditions for $f$, $f_\mathrm{i}$ and $f_s$ are:

$$\frac{df}{dz} = \frac{df_i}{dz} = \frac{df_i}{dz} = 0,\ \text{and} f = f_i = fs = 1 \ \text{ at } \ z = 0.$$

When an intense cosh-Gaussian laser beam propagates through the collisionless plasma, the background density of the plasma becomes modified due to ponderomotive force and relativistic effect. Therefore, the refractive index of the plasma increases and the laser beam gets focused in the plasma. Equations (16) and (17) give the intensity profile and beam width of cosh-Gaussian laser beam in plasma in the presence of relativistic and ponderomotive nonlinearities. The intensity profile of cosh-Gaussian laser beam depends on the beamwidth parameter ($f$). These equations have been solved for different laser and plasma parameters and the numerical results are presented in Figs. 1, 2, 3 and 4. The focusing/intensity of laser beam in plasma have been compared with only relativistic nonlinearity.

Figure 1 represents the variation of dimensionless beam width parameter ($f$) and laser beam intensity in collisionless plasma with the normalized propagation distance, when relativistic and ponderomotive nonlinearities and only relativistic nonlinearity are operatives. It is clear from Fig. 1a that beam width parameter ($f$) of cosh-Gaussian laser beam decreases earlier when both nonlinearities are operative and hence self-focusing becomes stronger. The total intensity of the beam depends upon the relativistic and ponderomotive nonlinearities introduced in the plasma; therefore, the intensity patterns in the relativistic regime is different from the ponderomotive and relativistic regime. It is obvious from Fig. 1b that the maximum intensity of laser beam gets enhanced by a factor of about 2.5 when both nonlinearities are operative.

Figure 2 shows the variation of dimensionless beam width parameter ($f$) and laser beam intensity in collisionless plasma with the normalized distance of propagation for different values of decentred parameter ($b$), when relativistic and ponderomotive nonlinearities are operative. At $b = 0$, the beam shows Gaussian nature. It is obvious from Fig. 2a that with the increase in the value of $b$, beam width parameter ($f$) of cosh-Gaussian laser beam is decreases. The extent of self-focusing of cosh-Gaussian laser beam increases with increase in $b$. Therefore, the intensity of the beam increases with increasing $b$ (Fig. 2b). Because Cosh-Gaussian beam converge earlier than Gaussian beam in plasma, so that this is one of the main reason to choose cosh-Gaussian profile of laser beam.

The variation of dimensionless beam width parameter ($f$) and laser beam intensity with the normalized distance of propagation for different values of relative plasma densities ($\omega_{p0}/\omega_0$) is depicted in Fig. 3. It is observed from the Fig. 3a, b that for higher value of relative plasma density, the extent of focusing and intensity of the beam increases. This is because ponderomotive nonlinearity enhances the self-focusing caused by relativistic nonlinearity. Furthermore, this is due to the weakening of diffractive term as compared to nonlinear refractive term in Eq. (17) at higher value of relative plasma density.

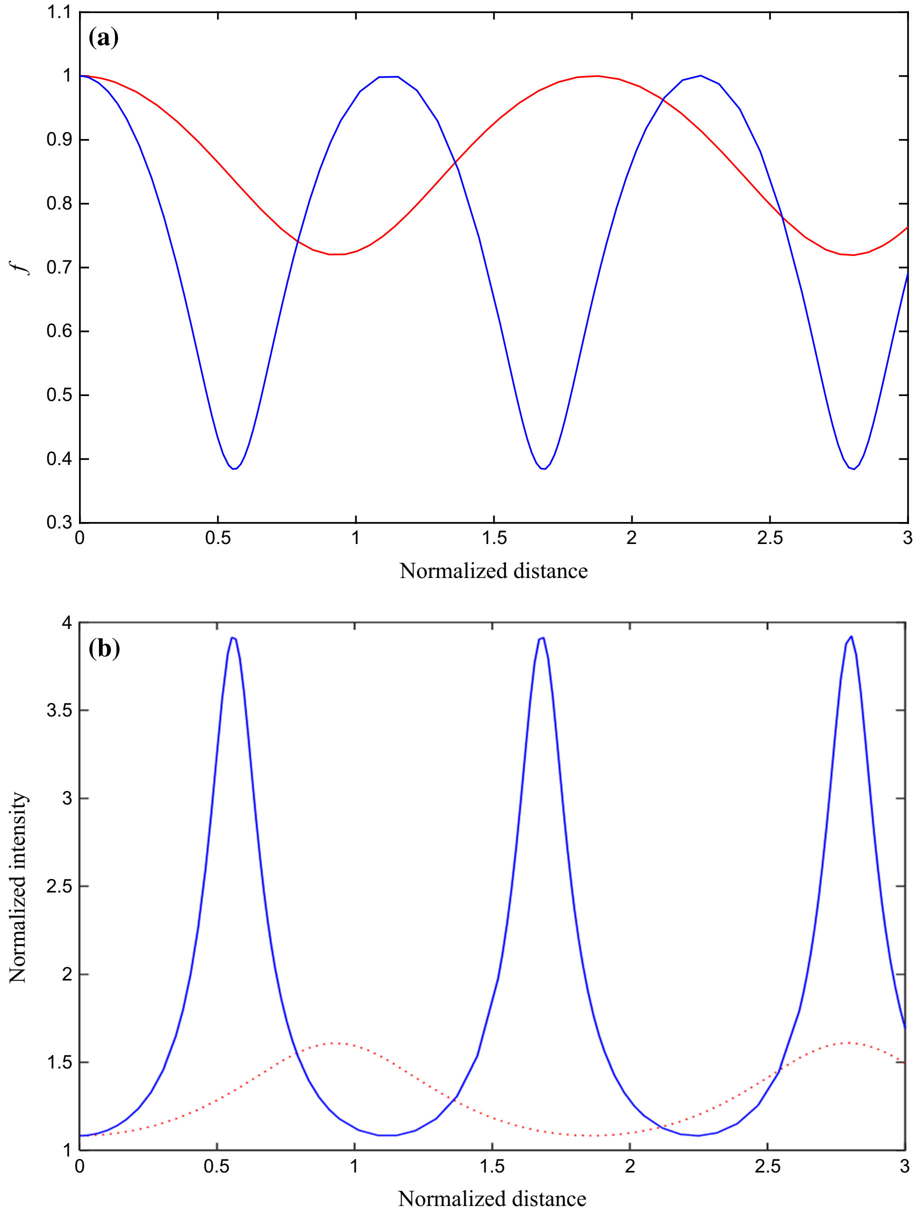


**Fig. 1** **a** Variation of the beamwidth parameter ($f$) of cosh-Gaussian laser beam with normalized propagation distance ($\xi$). **b** Variation in the normalized intensity of cosh-Gaussian laser beam with the normalized distance of propagation ($\xi$). Here $a = 1.4$, $b = 0.5$ and $\omega_{p0} = 0.28$. Red and blue colour curve are for only relativistic nonlinearity and relativistic-ponderomotive nonlinearity. (Color figure online)

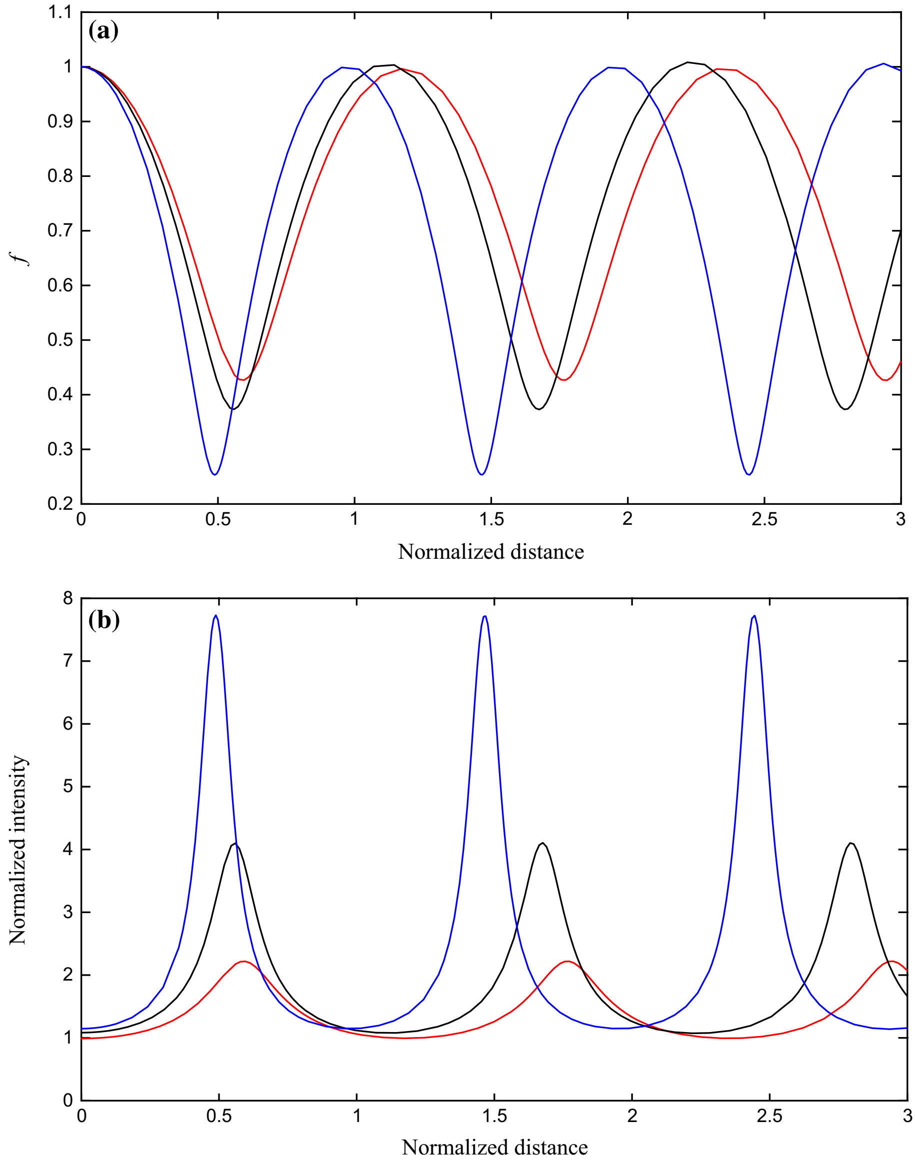


**Fig. 2** **a** Variation of beam width parameter ($f$) of cosh-Gaussian beam with the normalized distance ($\xi$) of propagation. **b** Variation in the normalized intensity of cosh-Gaussian laser beam with the normalized distance ($\xi$) of propagation for different values of decentred parameter $b$, when both relativistic and ponderomotive nonlinearities are operative. Here $a=1.4$ and $\omega_{p0}=0.28$. Red, black and blue colour curve are for $b=0$, 0.5 and 1 respectively. (Color figure online)

Figure 4 illustrates the variation of dimensionless beam width parameter ($f$) and laser beam intensity with the normalized distance of propagation for different values of incident laser intensities in collisionless plasma. It is evident from Fig. 4a that with the increase in the value of intensity parameter ($a$), beam width parameter increases and self-focusing

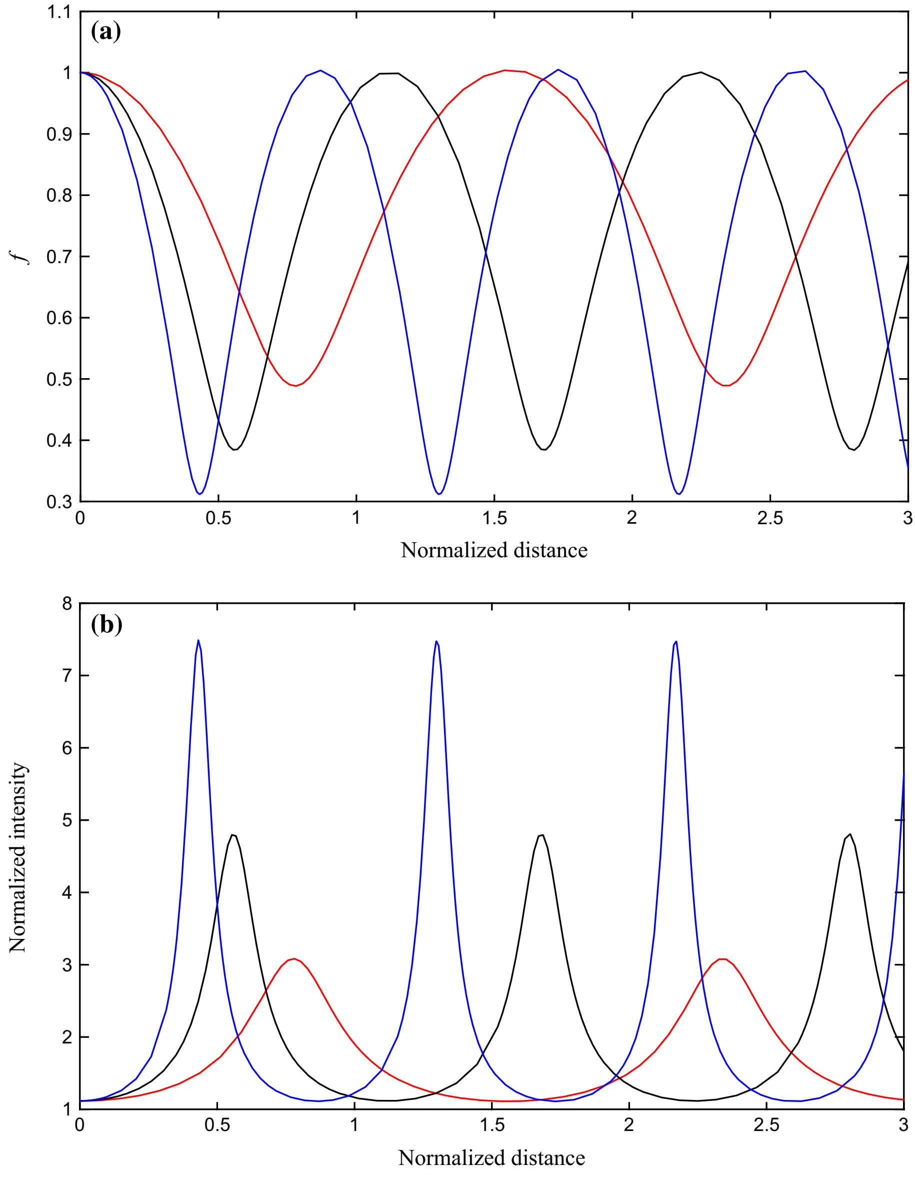


**Fig. 3** **a** Variation of beam width parameter ($f$) of cosh-Gaussian beam with the normalized distance ($\xi$) of propagation. **b** Variation in the normalized intensity of cosh-Gaussian laser beam with the normalized distance ($\xi$) of propagation for different values of $\omega_{p0}$, when both relativistic and ponderomotive nonlinearities are operative Here $b = 0.5$ and $a = 1.4$. Red, black and blue colour curve are for $\omega_{p0} = 0.18\ \omega_0$, $0.28\ \omega_0$ and $0.38\ \omega_0$ respectively. (Color figure online)

decreases. This behaviour of the laser is due to the fact that the incident laser intensity is very high i.e. more than $10^{18}$ W/cm$^2$. In addition, the nonlinear refractive term in Eq. (17) is sensitive to $a$ i.e the nonlinear refractive term becomes relatively weaker than diffractive term at higher values of $a$. However, when the values of $a < 10^{18}$ W/cm$^2$, focusing/intensity

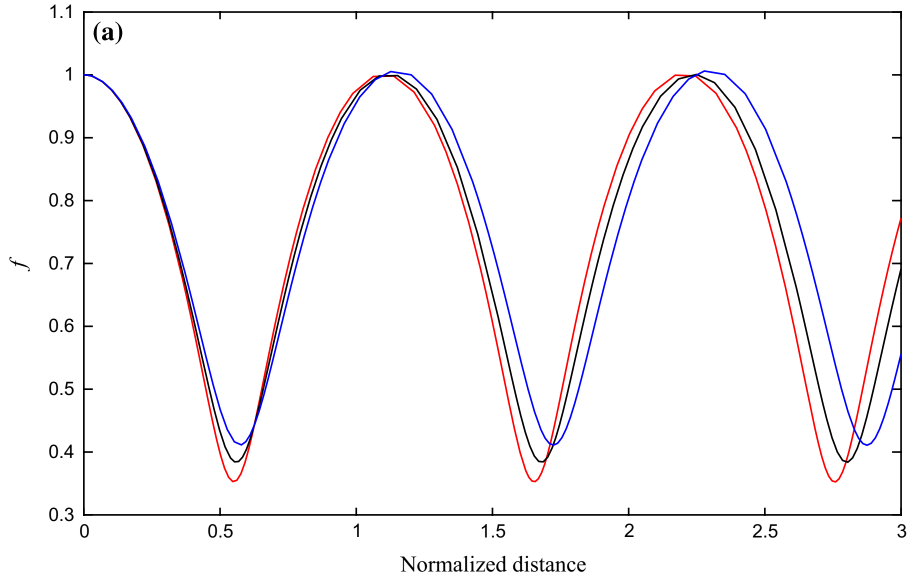


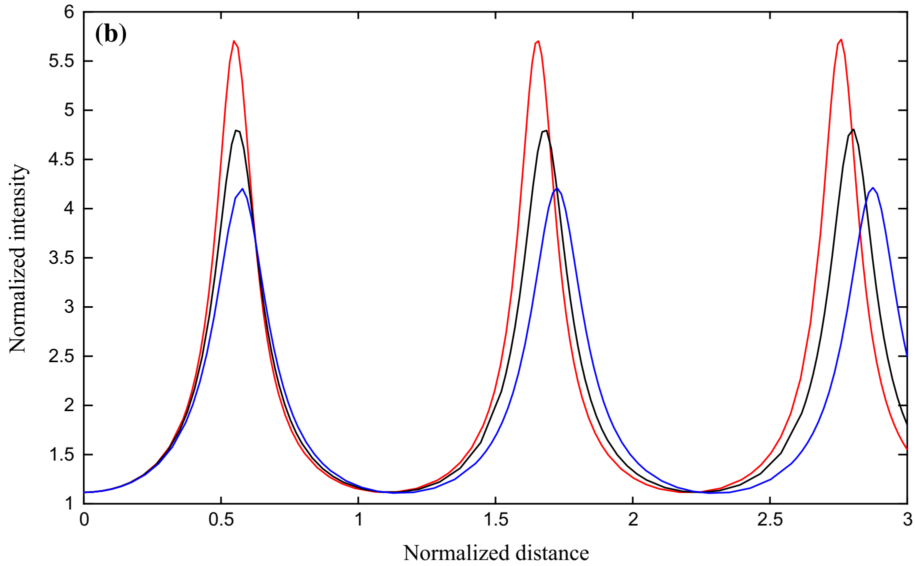


**Fig. 4** **a** Variation of beam width parameter ($f$) of cosh-Gaussian beam with the normalized distance ($\xi$) of propagation. **b** Variation in the normalized intensity of cosh-Gaussian laser beam with the normalized distance ($\xi$) of propagation for different values of $a$, when both relativistic and ponderomotive nonlinearities are operative. Here $b=0.5$ and $\omega_{p0}=0.28$. Red, black and blue colour curve are for $a=1$, 1.4 and 1.8 respectively. (Color figure online)

of cosh-Gaussian laser beam increases with increasing $a$ (Nanda and Kant 2014). Due to weak self-focusing, the normalized intensity of the cosh-Gaussian laser beam decreases at higher values of incident laser intensity (Fig. 4b).

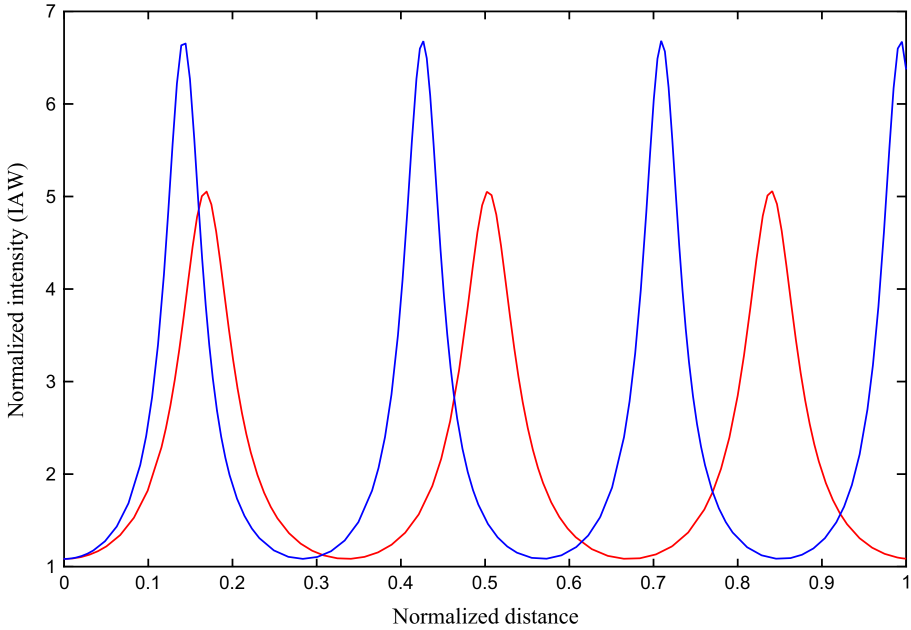


**Fig. 5** Variation in normalized intensity of ion-acoustic wave with normalized distance ($\xi$) of propagation for $a = 1.4$, $b = 0.5$ and $\omega_{p0} = 0.28$. Red and blue colour curve are for only relativistic nonlinearity and relativistic-ponderomotive nonlinearity. (Color figure online)

Equations (25) and (27) give the expression for density profile and the dimensionless beam width parameter ($f_i$) of ion-acoustic wave, when the coupling between self-focused cosh-Gaussian laser beam and ion-acoustic wave is taken into account. The amplitude of ion-acoustic wave depends upon the focusing of cosh-Gaussian laser beam and ion-acoustic wave in the plasma. We have solved Eq. (25) numerically with the help of Eq. (27) for different laser and plasma parameters to obtain the amplitude of the density perturbation at finite $z$ and the results are displayed in Figs. 5 and 6. Figure 5 represents the variation in the intensity of ion-acoustic wave with the normalized distance of propagation, when relativistic and ponderomotive nonlinearities and only relativistic nonlinearity are operatives. It is observed that the amplitude of excited ion-acoustic wave gets enhanced significantly when both nonlinearities are operative. Figure 6a-c shows the variation in the intensity of ion-acoustic wave with the normalized distance of propagation for different values of $b$, $\omega_{p0}/\omega_0$ and $a$ respectively, when both nonlinearities are operative. It is evident from Fig. 6a, b that the amplitude of ion-acoustic wave increases with increasing the values of $b$ and $\omega_{p0}/\omega_0$. This is due to strong focusing of main laser beam and ion-acoustic wave in the plasma. However, the amplitude of ion-acoustic wave decreases with increase in the value of incident laser intensity due to weak focusing of main laser beam and ion-acoustic wave (Fig. 6c).

In order to obtain the back reflectivity of stimulated Brillouin scattering (SBS) process, we have solved Eq. (45) numerically for different values of $b$, $\omega_{p0}/\omega_0$ and $a$ respectively. It is apparent from Eq. (45) that the back reflectivity of SBS is dependent

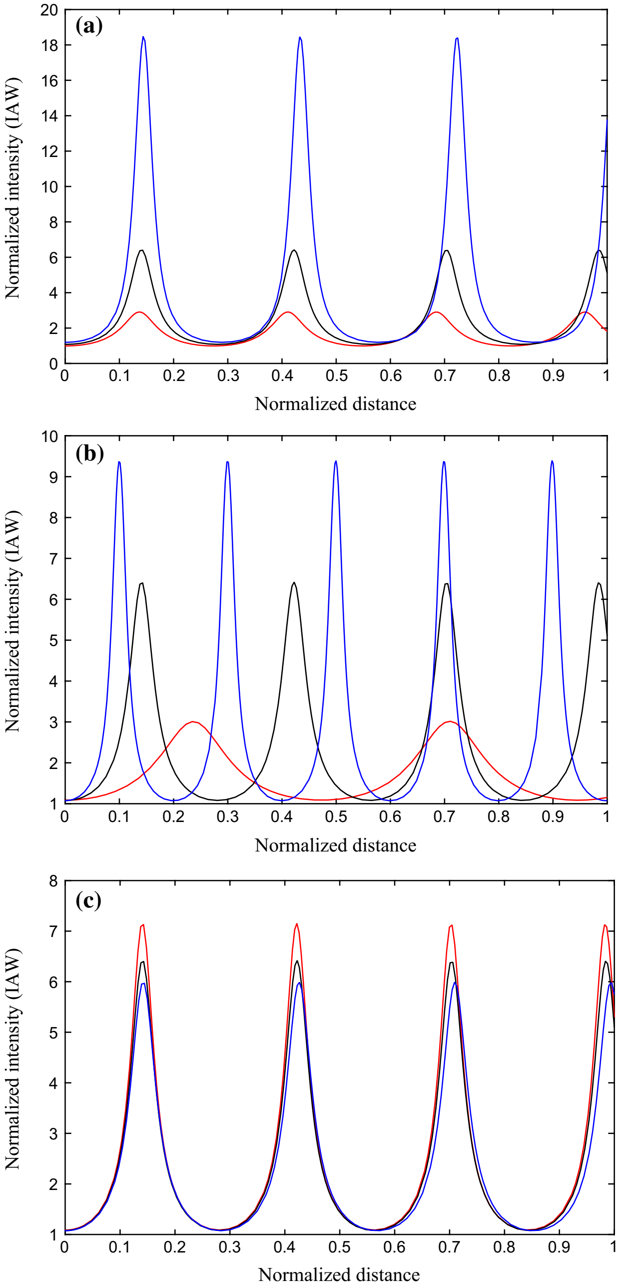


**Fig. 6** Variation in normalized intensity of ion-acoustic wave with normalized distance ($\xi$) of propagation for **a** different values of $b$ and constant value of $a=1.4$ and $\omega_{p0}=0.28$. Red, black and blue colour curve are for $b=0$, 0.5 and 1 respectively, **b** different values of $\omega_{p0}$ and constant value of $b=0.5$ and $a=1.4$. Red, black and blue colour curve are for $\omega_{p0}=0.18\ \omega_0$, $0.28\ \omega_0$ and $0.38\ \omega_0$ respectively, **c** different values of $a$ and constant values of $b=0.5$ and $\omega_{p0}=0.28$. Red, black and blue colour curve are for $a=1$, 1.4 and 1.8 respectively, when both relativistic and ponderomotive nonlinearities are taken into account. (Color figure online)

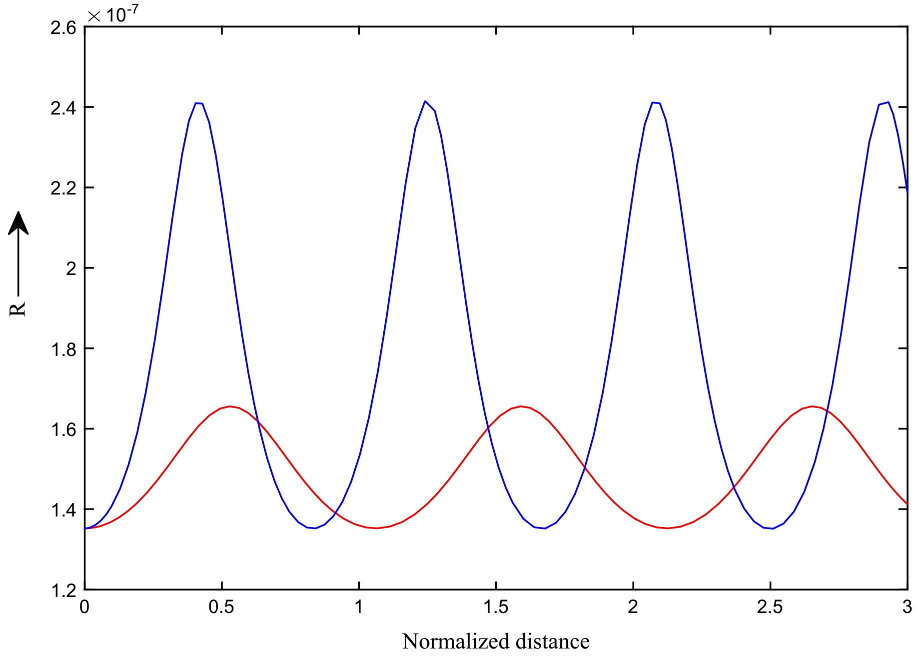


**Fig. 7** Variation of back reflectivity of SBS process with the normalized distance ($\xi$) of propagation for $a=1.4$, $b=0.5$ and $\omega_{p0}=0.28$. Red and blue colour curve are for only relativistic nonlinearity and relativistic-ponderomotive nonlinearity. (Color figure online)

on the intensity of IAW and the beam width of scattered wave. Figure 7 represent the variation in the back reflectivity of the SBS process with the normalized distance of propagation, when both relativistic and ponderomotive nonlinearities and only relativistic nonlinearity are operatives. It is evident from Fig. 7 that SBS back reflectivity enhanced when both nonlinearities are operative. This is mainly due to enhancement of intensity of main laser beam and ion-acoustic wave in plasma under relativistic-ponderomotive regime. Figure 8a–c depicts the variation in the back reflectivity of the SBS process with the normalized distance of propagation for different values of $b$, $\omega_{p0}/\omega_0$ and $a$, when relativistic and ponderomotive nonlinearities are operative. It is clear from the Fig. 8a, b that for higher values of $b$ and $\omega_{p0}/\omega_0$, the SBS back reflectivity gets enhanced. In addition, the back reflectivity decreases with increasing the value of incident laser intensity $a$ (Fig. 8c). This is because the focusing/intensity of main laser beam, ion-acoustic wave and the scattered wave increases with increasing the values of $b$ and $\omega_{p0}/\omega_0$, and decreases with increasing the value of $a$.

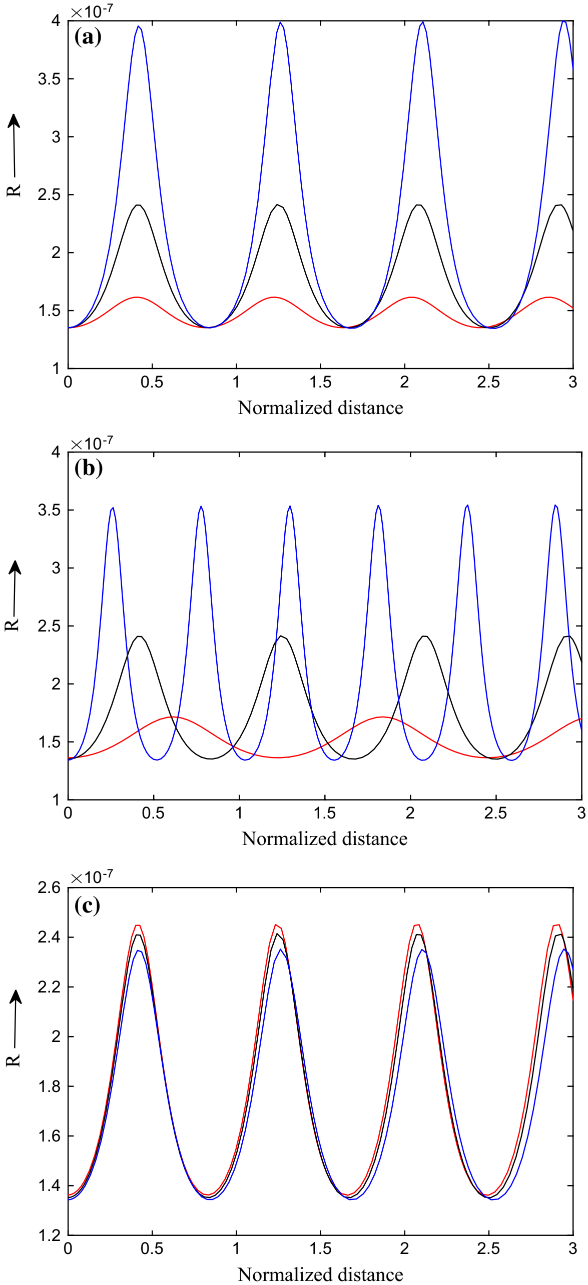


**Fig. 8** Variation of back reflectivity of SBS process with the normalized distance ($\xi$) of propagation for **a** different values of $b$ and constant value of $a=1.4$ and $\omega_{p0}=0.28$. Red, black and blue colour curve are for $b=0$, 0.5 and 1 respectively, **b** different values of $\omega_{p0}$ and constant value of $b=0.5$ and $a=1.4$. Red, black and blue colour curve are for $\omega_{p0}=0.18\ \omega_0$, $0.28\ \omega_0$ and $0.38\ \omega_0$ respectively, **c** different values of $a$ and constant values of $b=0.5$ and $\omega_{p0}=0.28$. Red, black and blue colour curve are for $a=1$, 1.4 and 1.8 respectively, when both relativistic and ponderomotive nonlinearities are taken into account. (Color figure online)

## 6 Conclusions

In summary, we have studied self-focusing of cosh-Gaussian laser beam in collisionless plasma and its effect on the generation of ion-acoustic wave and back reflectivity of stimulated Brillouin scattering, when both relativistic and ponderomotive nonlinearities are operative. Under WKB and paraxial-ray approximations, an analytical model have been developed for stimulated Brillouin back scattering of self-focused cosh-Gaussian laser beam in a collisionless plasma and proceeded by numerical computation. The results are compared with relativistic nonlinearity. The focusing/intensity of laser beam and ion-acoustic wave becomes enhanced in the presence of relativistic and ponderomotive nonlinearities. We have examined the effect of various laser and plasma parameters viz. decentred parameter ($b$), relative plasma density ($\omega_{p0}/\omega_0$) and incident laser intensity ($a$) on the focusing/intensity of cosh-Gaussian laser beam and ion-acoustic wave as well as back reflectivity of SBS process. It is found that the extent of focusing/intensity of laser beam and ion-acoustic wave and back reflectivity of SBS increases with increasing the value of $b$ and $\omega_{p0}/\omega_0$. The back reflectivity gets enhanced in the presence of relativistic and ponderomotive nonlinearities. In addition, the back reflectivity of the scattered wave gets suppressed at higher value of $a$. This is because the focusing/intensity of the laser beam and ion-acoustic wave decrease with increasing the value of $a$. The results of the present study are useful in laser-induced fusion scheme where SBS plays a very important role.

**Acknowledgements** The authors are thankful to the Science and Engineering Research Board (SERB), Department of Science and Technology, Government of India for providing financial assistance for carrying out this research work vide project file No. EMR/2016/000112.

## References

Akhmanov, S.A., Sukhorukov, A.P., Khokhlov, R.V.: Self-focusing and diffraction of light in a nonlinear medium. Sov. Phys. Usp. **10**(5), 609–636 (1968)

Albright, B.J., Yin, L., Bowers, K.J., Bergen, B.: Multi-dimensional dynamics of stimulated Brillouin scattering in a laser speckle: ion acoustic wave bowing, breakup, and laser-seeded two-ion-wave decay. Phys. Plasmas **23**(3), 032703 (2016)

Aleksandrov, V.V., Brenner, M.V., Koval'skii, N.G., Loburev, S.V., Rubenchik, A.M.: Brillouin scattering in a laser plasma at moderate intensities 1012-1014 W/cm$^2$. Sov. Phys. JETP **61**(3), 459–463 (1985)

Al-Rashed, A.A.R., Saleh, B.E.A.: Decentered Gaussian beams. Appl. Opt. **34**(30), 6819–6825 (1995)

Amin, M.R., Capjack, C.E., Frycz, P., Rozmus, W., Tikhonchuk, V.T.: Two-dimensional studies of stimulated Brillouin scattering, filamentation, and self-focusing instabilities of laser light in plasmas. Phys. Fluids B **5**(10), 3748–3764 (1993)

Baldis, H.A., Villeneuve, D.M., La Fontaine, B., Enright, G.D., Labaune, C., Baton, S., Mounaix, P., Pesme, D., Casanova, M., Rozmus, W.: Stimulated Brillouin scattering in picosecond time scales: experiments and modelling. Phys. Fluids B **5**(9), 3319–3327 (1993)

Baton, S.D., Amiranoff, F., Malka, V., Modena, A., Salvati, M., Coulaud, C., Rousseaux, C., Renard, N., Mounaix, P.H., Stenz, C.: Measurement of the stimulated Brillouin scattering reflectivity from a spatially smoothed laser beam in a homogeneous large-scale plasma. Phys. Rev. E **57**(5), R4895 (1998)

Borisov, A.M., Borovskiy, A.V., Shiryaev, O.B., Korobkin, V.V., Prokhorov, A.M.: Relativistic and charge-displacement self-channeling of intense ultrashort laser pulses in plasmas. Phys. Rev. A **45**(8), 5830 (1992)

Brandi, H.S., Manus, C., Mainfray, G.: Relativistic self-focusing of ultraintense laser pulses in inhomogeneous underdense plasmas. Phys. Rev. E **47**(5), 3780 (1993a)

Brandi, H.S., Manus, C., Mainfray, G.: Relativistic and ponderomotive self-focusing of a laser beam in a radially inhomogeneous plasma. I. Paraxial approximation. Phys. Fluids B **5**(10), 3539–3550 (1993b)

Casperson, L.W., Hall, D.G., Tovar, A.A.: Sinusoidal-Gaussian beams in complex optical systems. J. Opt. Soc. Am. A **14**(12), 3341–3348 (1997)

Chirokikh, A., Seka, W., Simon, A., Craxton, R.S., Tikhonchuk, V.T.: Stimulated Brillouin scattering in long-scale-length laser plasmas. Phys. Plasmas **5**(4), 1104–1109 (1998)
Eliseev, V.V., Rozmus, W., Tikhonchuk, V.T., Capjack, C.E.: Stimulated Brillouin scattering and ponderomotive self-focusing from a single laser hot spot. Phys. Plasmas **2**(5), 1712–1724 (1995)
Fuchs, J., Labuane, C., Depierreux, D., Baldis, H.A., Michard, A., James, G.: Experimental evidence of plasma-induced incoherence of an intense laser beam propagating in an underdense plasma. Phys. Rev. Lett. **86**(3), 432–435 (2001)
Gao, W., Lu, Z.W., Wang, S.Y., He, W.M., Hasi, W.L.J.: Measurement of stimulated Brillouin scattering threshold by the optical limiting of pump output energy. Laser Part. Beams **28**(1), 179–184 (2010)
Gauniyal, R., Ahmad, N., Rawat, P., Gaur, B., Mahmoud, S.T., Purohit, G.: Stimulated Brillouin backscattering of hollow Gaussian laser beam in collisionless plasma under relativistic–ponderomotive regime. Laser Part. Beams **35**(1), 81–91 (2017)
Gill, T.S., Mahajan, R., Kaur, R.: Self-focusing of cosh-Gaussian laser beam in a plasma with weakly relativistic and ponderomotive regime. Phys. Plasmas **18**(3), 033110 (2011)
Giulietti, A., Macchi, A., Schifano, E., Biancalana, V., Danson, C., Giulietti, D., Gizzi, L.A., Willi, O.: Stimulated Brillouin backscattering from underdense expanding plasmas in a regime of strong filamentation. Phys. Rev. E **59**(1), 1038–1046 (1999)
Gupta, N., Singh, A.: Dynamics of quadruple laser beams in collisionless plasmas. Waves Random Complex Media **28**, 1–18 (2017)
Habibi, M., Ghamari, F.: Significant enhancement in self-focusing of high-power laser beam through dense plasmas by ramp density profile. J. Opt. Soc. Am. B **32**(7), 1429–1434 (2015)
Huller, S., Masson-Laborde, P.E., Pesme, D., Labaune, C., Bandulet, H.: Modeling of stimulated Brillouin scattering in expanding plasmas. J. Phys. Conf. Ser. **112**(2), 022031 (2008)
Kaw, P.K., Schmidt, G., Wilcox, T.: Filamentation and trapping of electromagnetic radiation in plasmas. Phys. Fluids **16**(9), 1522–1525 (1973)
Konar, S., Mishra, M., Jana, S.: Nonlinear evolution of cosh-Gaussian laser beams and generation of flat top spatial solitons in cubic quintic nonlinear media. Phys. Lett. A **362**(5–6), 505–510 (2007)
Krall, N.A., Trivelpicec, A.W.: Principle of Plasma Physics. McGraw Hill-Kogakusha, Tokyo (1973)
Kruer, W.L.: The Physics of Laser Plasma Interactions. Addison-Wesley, Redwood City (1988)
Labaune, C., Fabre, E., Michard, A., Briand, F.: Evidence of stimulated Brillouin backscattering from a plasma at short laser wavelengths. Phys. Rev. A **32**(1), 577 (1985)
Labaune, C., Rozmus, W., Baldis, H.A., Mounaix, P., Pesme, D., Baton, S.D., Fontaine, B.L., Villeneuve, D.M., Enright, G.D.: Proceedings of SPIE 1413, Short-Pulse High-Intensity Lasers and Applications (1991)
Labaune, C., Baldis, H.A., Schifano, E., Bauer, B.S., Michard, A., Renard, N., Seka, W., Moody, J.D., Estabrook, K.G.: Location of ion-acoustic waves from back and side stimulated Brillouin scattering. Phys. Rev. Lett. **76**(20), 3727 (1996)
Labaune, C., Baldis, H.A., Renard, N., Schifano, E., Michard, A.: Interplay between ion acoustic waves and electron plasma waves associated with stimulated Brillouin and Raman scattering. Phys. Plasmas **4**(2), 423–427 (1997)
Lu, B., Luo, S.: Beam propagation factor of hard-edge diffracted cosh-Gaussian beams. Opt. Commun. **178**(4–6), 275–281 (2000)
Lu, B., Ma, H., Zhang, B.: Propagation properties of cosh-Gaussian beams. Opt. Commun. **164**(4–6), 165–170 (1999)
Mahmoud, S.T., Sharma, R.P., Kumar, A., Yadav, S.: Effect of pump depletion and self-focusing on stimulated Brillouin scattering process in laser-plasma interactions. Phys. Plasmas **6**(3), 927–931 (1999)
Masson-Laborde, P.E., Hüller, S., Pesme, D., Labaune, Ch., Depierreux, S., Loiseau, P., Bandulet, H.: Stimulated Brillouin scattering reduction induced by self-focusing for a single laser speckle interacting with an expanding plasma. Phys. Plasmas **21**(3), 032703 (2014)
Mounaix, P., Divol, L., Huller, S., Tikhonchuk, V.T.: Effects of spatial and temporal smoothing on stimulated Brillouin scattering in the independent-hot-spot model limit. Phys. Rev. Lett. **85**(21), 4526–4529 (2000)
Myatt, J., Pesme, D., Huller, S., Maximov, A.V., Rozmus, W., Capjack, C.E.: Nonlinear propagation of a randomized laser beam through an expanding plasma. Phys. Rev. Lett. **87**(25), 255003 (2001)
Nanda, V., Kant, N.: Strong self-focusing of a cosh-Gaussian laser beam in collisionless magneto-plasma under plasma density ramp. Phys. Plasmas **21**(7), 072111 (2014)
Neumayer, P., Berger, R.L., Divol, L., Froula, D.H., London, R.A., MacGowan, B.J., Meezan, N.B., Ross, J.S., Sorce, C., Suter, L.J., Glenzer, S.H.: Suppression of stimulated Brillouin scattering by increased Landau damping in multiple-ion-species hohlraum plasmas. Phys. Rev. Lett. **100**(10), 105001 (2008)

Niknam, A.R., Barzegar, S., Hashemzadeh, M.: Self-focusing and stimulated Brillouin back-scattering of a long intense laser pulse in a finite temperature relativistic plasma. Phys. Plasmas **20**, 122117 (2013)
Purohit, G., Rawat, P.: Stimulated Brillouin backscattering of a ring-rippled laser beam in collisionless plasma. Laser Part. Beams **33**(3), 499–509 (2015)
Rozmus, W., Sharma, R.P., Samson, J.C., Tighe, W.: Nonlinear evolution of stimulated Raman scattering in homogeneous plasmas. Phys. Fluids **30**(7), 2181–2193 (1987)
Sharma, R.P., Sharma, P., Rajput, S., Bhardwaj, A.K.: Suppression of stimulated Brillouin scattering in laser beam hot spots. Laser Part. Beams **27**(4), 619–627 (2009)
Singh, A., Walia, K.: Self-focusing of Gaussian laser beam in collisionless plasma and its effect on stimulated Brillouin scattering process. Opt. Commun. **290**, 175–182 (2013)
Sodha, M.S., Ghatak, A.K., Tripathi, V.K.: Self-focusing of Laser Beams. Tata-McGraw-Hill, New Delhi (1974)
Thakur, V., Kant, N.: Stronger self-focusing of cosh-Gaussian laser beam under exponential density ramp in plasma with linear absorption. Optik **183**, 912–917 (2019)
Varaki, M.A., Jafari, S.: Relativistic self-focusing of an intense laser pulse with hot magnetized plasma in the presence of a helical magnetostatic wiggler. Phys. Plasmas **24**, 082309 (2017)
Wang, Y.L., Lu, Z.W., He, W.M., Zheng, Z.X., Zhao, Y.H.: A new measurement of stimulated Brillouin scattering phase conjugation fidelity for high pump energies. Laser Part. Beams **27**(2), 297–302 (2009)
Wei, M.S., Beg, F.N., Clark, E.L., Dangor, A.E., Evans, R.G., Gopal, A., Ledingham, K.W.D., McKenna, P., Norreys, P.A., Tatarakis, M., Zepf, M., Krushelnick, K.: Observations of the filamentation of high-intensity laser-produced electron beams. Phys. Rev. E **70**(5), 056412 (2004)
Yahia, V., Masson-Laborde, P.E., Depierreux, S., Goyon, C., Loisel, G., Baccou, C., Borisenko, N.G., Orekhov, A., Rienecker, T., Rosmej, O., Teychenné, D., Labaune, C.: Reduction of stimulated Brillouin backscattering with plasma beam smoothing. Phys. Plasmas **22**(4), 042707 (2015)
Zhou, G.: Propagation of a higher-order cosh-Gaussian beam in turbulent atmosphere. Opt. Express **19**(5), 3945–3951 (2011)